**Atmospheric
Chemistry
and Physics**

Meteoroid velocity distribution derived from head echo data collected at Arecibo during regular world day observations

M. P. Sulzer

Arecibo Observatory, Arecibo, Puerto Rico

Abstract. We report the observation and analysis of ion-
ization flashes associated with the decay of meteoroids (so-
called head echos) detected by the Arecibo 430 MHz radar
during regular ionospheric observations in the spring and au-
tumn equinoxes. These two periods allow pointing well-
above and nearly-into the ecliptic plane at dawn when the
event rate maximizes. The observation of many thousands of
events allows a statistical interpretation of the results, which
show that there is a strong tendency for the observed mete-
oroids to come from the apex as has been previously reported
(Chau and Woodman, 2004). The velocity distributions agree
with Janches et al. (2003a) when they are directly compara-
ble, but the azimuth scan used in these observations allows
a new perspective. We have constructed a simple statistical
model which takes meteor velocities as input and gives radar
line of sight velocities as output. The intent is to explain
the fastest part of the velocity distribution. Since the speeds
interpreted from the measurements are distributed fairly nar-
rowly about nearly $60 \, \mathrm{km \, s^{-1}}$, double the speed of the earth
in its orbit, is consistent with the interpretation that many of
the meteoroids seen by the Arecibo radar are moving in or-
bits about the sun with similar parameters as the earth, but in
the retrograde direction. However, it is the directional infor-
mation obtained from the beam-swinging radar experiment
and the speed that together provide the evidence for this in-
terpretation. Some aspects of the measured velocity distribu-
tions suggest that this is not a complete description even for
the fast part of the distribution, and it certainly says nothing
about the slow part first described in Janches et al. (2003a).
Furthermore, we cannot conclude anything about the entire
dust population since there are probably selection effects that
restrict the observations to a subset of the population.

Correspondence to: M. P. Sulzer
(msulzer@naic.edu)

1 Introduction

The Arecibo 430 MHz radar is a very powerful and sensitive
instrument used primarily for measurements of incoherent
scatter (IS) in the earth's ionosphere. In the last several years
it has been used for the observation of small meteoroids as
they penetrate into the atmosphere, depositing sufficient en-
ergy to cause detectable ionization in the immediate region
of the decaying meteoroid resulting from collisions with at-
mospheric particles. The result is the so-called head echo,
which is not yet well understood. The Arecibo instrument
is one of several high-sensitivity radars providing these mea-
surements (see the list of references in Chau and Woodman,
2004). Most of these observations have used observational
techniques designed especially for observation of the very
brief flashes of ionization associated with the collisions. It is
possible to use much data intended for ionospheric observa-
tions to detect the decay of the meteoroids and measure some
of the associated parameters, such as the time of the flash, its
intensity, its altitude, and the velocity component along the
radar line of sight. However, it is necessary to have access
to the raw voltage samples, not the analyzed data. We used
a high resolution mode intended for measuring the IS spec-
trum in the E region of the ionosphere. The spectral width of
the IS ion line is much less than the Doppler shifts of most
of the head echos, and so in this case the wide bandwidth
used to obtain good range resolution allows observation of
the head echos, which have very narrow spectra located at
large Doppler shifts. Most current IS measurements made
at Arecibo sample the necessary bandwidth even if the res-
olution is not necessary, and so most of the data are at least
potentially suitable for analysis of meteor head echos. How-
ever, the coded long pulse technique used for observations
described here is particularly well-suited because the appro-
priate analysis makes it very easy to locate the meteoroid
path in height and frequency.
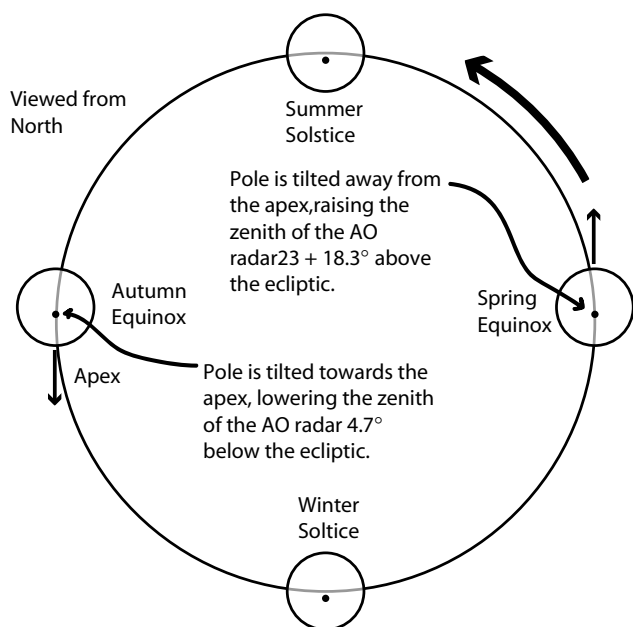
Fig. 1. The location of the radar with respect to the ecliptic plane as a function of the season.

Fig. 2. This drawing shows that the repetiton period of a target located in the north (or south) is twice as high as a target located in the east (or west).

We present results from two periods, the spring and autumn equinoxes. The Arecibo radar cannot point more than $20°$ from the zenith, and sensitivity issues restrict the pointing in these ionospheric observations to $15°$. As meteor observations have previously, we augment this range by using the seasonal changes of the location of the radar with respect to the ecliptic plane. Figure 1 shows that in the spring the radar zenith is well above the ecliptic at dawn, while in the fall it lies almost in it, and so points nearly along the apex as the meteor event rate maximizes. These differences in pointing have important consequences for the observations.

We have a sufficiently large number of events so that we can make conclusions requiring statistical analysis, and we see the previously-reported tendency for the apparent source of the meteoroids to lie along the apex defined by the motion of the earth around the sun (Chau and Woodman, 2004). The speeds computed from our measurements are distributed fairly narrowly just under $60\,\mathrm{km\,s^{-1}}$. Since this is nearly double the speed of the earth in its orbit, the obvious interpretation, given the directional information, is that most of the meteoroids seen by the Arecibo radar are moving in orbits about the sun with similar parameters as the earth, but in the retrograde direction. We do not even claim this as a potential description for the complete population, since we currently have no way to remove certain observational biases, and it is not clear how much information would be available from a much larger set of data after the application of careful modeling. A weaker distribution of slower particles is seen in the fall observations, and possibly in the spring observations. This was first reported by Janches et al. (2003a).
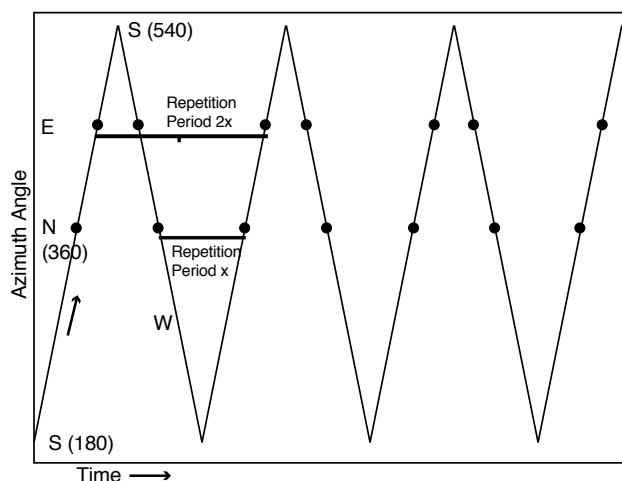
We have constructed a simple statistical model intended to show that the above interpretation is consistent with the general properties of the fastest part of the observed velocity distribution. It is not an accurate model intended for parameter fitting, but is only a first step in this direction. This interpretation helps explain why meteors seem to come "down the beam" at Arecibo. This question is discussed in Janches et al. (2003a) and Janches et al. (2003b), which favor an interpretation based on atmospheric effects. Our interpretation does not exclude atmospheric effects; in fact, we have had to assume such an effect to make it work.

2 Experiment Description

The ionospheric experiment that provided the data for the meteor observations we describe here is one mode of Arecibo's World Day observations. The pointing angle from the zenith (zenith angle, or α_{za}) is fixed at $15°$, while the azimuth angle (α_{az}), measured from north in the eastward direction, is varied. Ideally, the azimuth angle would continue to increase at the maximum (slew) rate, but in practice it is necessary to stop and turn around so that cables carrying power and information do not break. The procedure is to scan from $180°$ (looking south with the line feed) to $540°$, a complete revolution. Then the motion stops, and the pointing returns to $180°$. It is necessary to account for the time spent motionless at the limits of the motion and accelerating near the limits in some of the data analysis described later.

Figure 2 shows an important consequence of the pattern of azimuth motion. A target located in the north or south would be sampled uniformly with an interval of $180°$ (about 8 min). However, a target located in the east or west has a fundamental period of about 16 min, but the time series would also
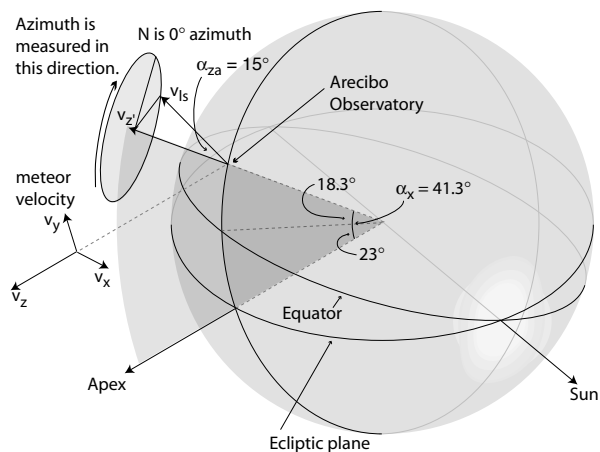
Fig. 3. Observations during the Spring Equinox at dawn. The radar and the apex define a plane perpendicular to the ecliptic.

Fig. 4. Computing the radar line of sight velocity from a velocity vector $\mathbf{v}'$.

have additional periods resulting from the alternating short and long intervals between samples. The time series of a parameter associated with a target such as line of sight velocity shows this effect also.

Figure 3 shows in detail the spring conditions corresponding to the rightmost part of Fig. 1. At dawn when the projection of the radar zenith in the ecliptic plane points into the apex, the zenith pointing position is $41.3°$ north of the ecliptic.

It is convenient to express the meteor velocities in a coordinate system where the z-axis points to the apex, where the x-axis points in the eastward direction in the ecliptic plane, and where the y-axis points northward perpendicular to the ecliptic plane. It is also convenient to find the radar line-of-sight velocities as a function of the x, y, and z components. The first step in this process is to define a $x'y'z'$ system by rotating about the x-axis so that the z' axis is parallel to the radar zenith. The velocity transformation is

$$
\begin{vmatrix} v'_x \\ v'_y \\ v'_z \end{vmatrix} = \begin{vmatrix} 1 & 0 & 0 \\ 0 & \cos\alpha_x & -\sin\alpha_x \\ 0 & \sin\alpha_x & \cos\alpha_x \end{vmatrix} \begin{vmatrix} v_x \\ v_y \\ v_z \end{vmatrix},
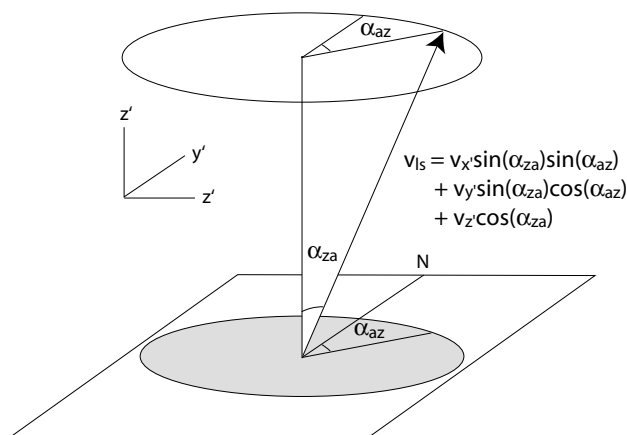\tag{1}
$$

where α_x is defined in Fig. 3

Figure 4 shows the transformation to the line-of-sight velocity v_{ls}. The transformation is

$$
v_{ls} = v'_x \sin\alpha_{za} \sin\alpha_{az}
\tag{2}
$$
$$
+ v'_y \sin\alpha_{za} \cos\alpha_{az} + v'_z \cos\alpha_{za}.
$$

The flat plane in Fig. 4 would be tangent to the sphere of Fig. 3 at the location of the Arecibo Observatory.

At times other than dawn, the radar no longer lies in the yz plane, and since the angle between the equator and ecliptic changes, α_x is a function of time. Also there is a rotation about the y axis. We do not need to consider this more general transformation in detail.

The observations used a radar pulse $400\,\mu$s in length; the pulse modulation was binary phase using a pseudo-random phase sequence with a baud length of $2\,\mu$s, and the transmission used a different code for each pulse. Sulzer (1986) describes the application of this technique to IS. In that application the signal has a correlation time that is shorter than the pulse length, and the technique allows the measurement of the signal autocorrelation function with range resolution equal to the baud length of the code. However, the correlation time is much longer than the inverse of the baud length (narrow spectrum), and it is possible to speed up the calculations for the IS spectrum while losing the possibility of measuring the meteor parameters by failing to calculate the full bandwidth. Thus it is necessary to perform an independent analysis for the meteors. This analysis takes longer than real time, but it is nonetheless convenient because the raw voltage samples are stored on disk for some time after the experiment.

The spring experiment used the line feed only, while the fall used both the line feed and Gregorian. The presentation here includes only the linefeed data, since the analysis of the Gregorian data is not complete.

The inter-pulse period of this experiment is $10\,\mu$s; this is longer than one would like for a detailed analysis of the head echo, but perfectly satisfactory for counting powers, heights, and frequencies. Meteors are occasionally seen for as long as five inter-pulse periods, but often are visible for only one.

There are two possible ways to analyze the raw data. The first is the standard coded long pulse analysis in which one multiplies the code into the data samples beginning at some point, which defines the decoded range. One computes the power spectrum of the product, and does this for each
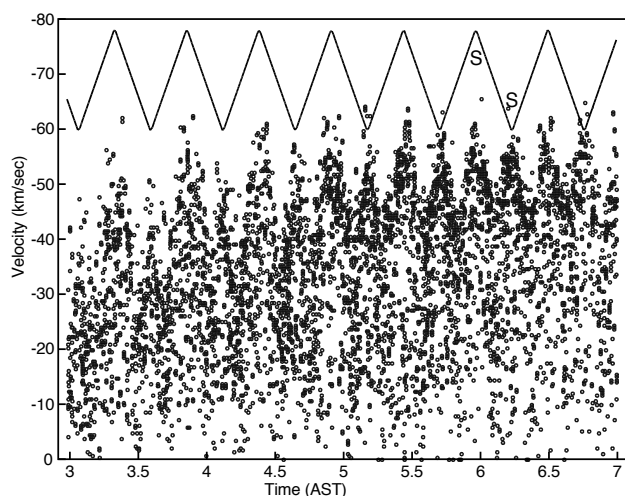
Fig. 5. The velocities of all meteoroids on 20 March 2003 from 03:00 to 07:00 AST.
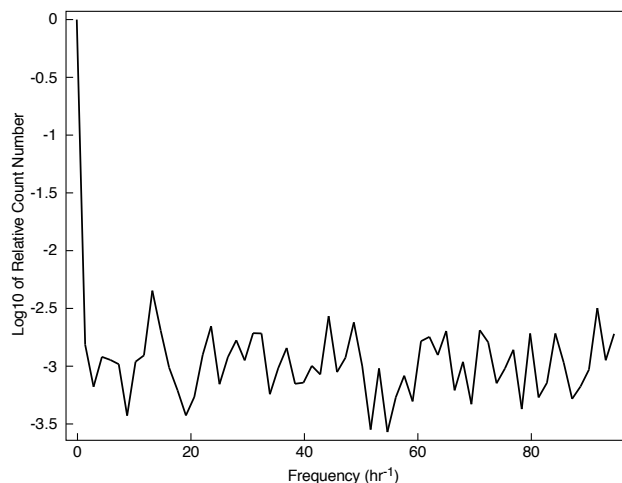
Fig. 6. The power spectrum of the function formed by binning the detections by azimuth. The result is the average of the four days, 20–23 March 2003, covering the time period 4.6 to 6.1 AST.

possible range. The other method is to decode the time sequence as one would for a power profile, but to repeat the decoding on frequency shifted versions of the signal. It turns out that the two methods treat a single meteor signal in nearly identical ways, but the processing of the overlapping of multiple signals is different. However, even two meteors at once is a rare event, and the ionospheric clutter cannot be decoded in any case since its correlation time is too short. The first analysis is a simple modification of the standard ionospheric analysis, making sure that the high Doppler shifts are not discarded in order to speed up the computations, and it guarantees that the ionospheric clutter is randomized, the best available option if it cannot be eliminated. Thus we chose the first method.

The analysis is divided into two steps, and the results of the first step are saved since it is convenient to redo the second in different ways as required. The first step computes the spectra for all ranges for the samples from a single radar pulse. It is not possible to save these spectra, since they require more storage space than the original samples, but since we expect either no detection or the detection of a single meteor, we find the maximum power in any of the spectra and save its range, frequency, and intensity as well as time and pointing information. We do this for the received power from each radar pulse.

The second step is to find which of the saved maxima are meteor detections and which are noise. This involves finding a threshold in which the majority of the events define a baseline from which the few deviate. We use a sliding time interval since the noise level is a function of time. The analysis would have been easier if we saved an average noise level for reach radar pulse in the first step, but this would make little difference in the results during the night and around dawn, the time period used in this paper.

3 Spring Observations

The spring observations occurred on four days near the spring equinox of 2003. We concentrate on the four dawn periods since the meteor count is maximum at this time. Figure 5 shows the velocities versus time of all detected events from 03:00 to 07:00 AST on 20 March 2003. Each event is a small dot; the solid line indicates the azimuth positions. Note that near dawn there is a periodic ripple in the maximum velocity which is locked in phase to the azimuth motion, and that the maximum velocity occurs when the azimuth is pointed to the south. When the radar points south, its projection along the apex is at its maximum, and so Fig. 5 is consistent with velocities aligned along the apex, at least approximately.

Several hours before dawn the ripples have half the frequency. This is because an apex-aligned feature has a significant east-west component before dawn. As explained in Sect. 2 east-west features have twice the period, or half the frequency of north-south features. Obviously the ripple is complicated, and we will not try to determine its exact shape.

This tentative conclusion of alignment with the apex would be doubtful if there were some selection effect, perhaps instrumental, which emphasized different parts of the population as a function of azimuth angle. Such a bias would likely be revealed by the event count rate as a function of azimuth angle. Figure 6 shows a power spectrum of the series obtained by by finding the event counts in 128 uniformly spaced azimuth bins. The plot shows the sum of the results from four dawn periods from 4.6 to 6.1 AST. The dates are the 20–23 March 2003. The result is almost what one would expect from random variations only in the count rate. The zero frequency peak indicates the total count rate, and there is only one other peak that might be significant, and it does
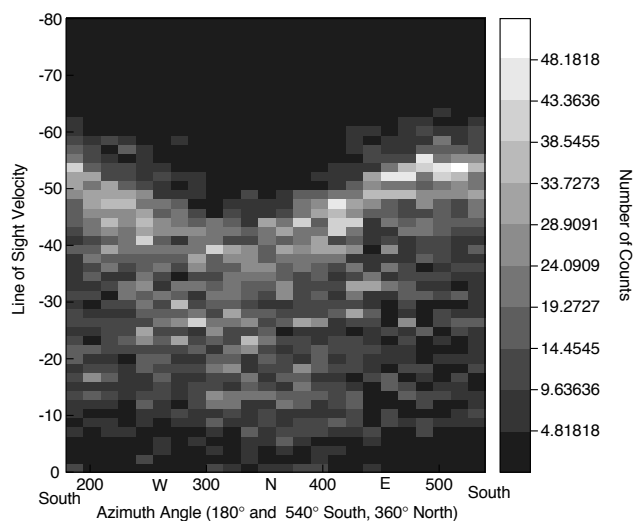
Fig. 7. The distribution of the velocities with azimuth angle from four days of spring equinox data (20–23 March 2003).

Fig. 8. Constant azimuth cuts at the maximum and minimum from the results of the previous figure.

not lie at a harmonic of the rotation time. We conclude that there are no significant biases which would show up in an analysis of the count rates.

Figure 7 shows the results of putting the line-of-sight velocities from 20–23 March 2003 into 24 azimuth bins. The maximum is not centered exactly in the southern direction as one might (mistakenly) expect from Fig. 5. This effect is significant since it is visible in the individual days after azimuth binning. The depth of the minimum in approximately the northern direction provides a method to see if the center of the velocity distribution lies in the ecliptic plane, as we can show using the analysis of Sect. 2.

Figure 8 shows two cuts in the velocity direction from Fig. 7. The dark thin line is from the maximum (nearly south); it has a high peak in the distribution. The thicker gray line is from 180° away; it is less highly peaked. This indicates that there is dispersion in the velocity component in the y direction (perpendicular to the ecliptic).

To further demonstrate the plausibility of the interpretation involving alignment with the apex, we have computed an approximate statistical model using the transformation between the meteor velocity and the line of sight velocity of Sect. 2. In the model we assume that meteoroids initially have a speed of $60\,\mathrm{km\,s^{-1}}$, that they have some average and random (Gaussian distributed) x and y velocities, and that the speed decreases by a random amount (χ-square distribution with one degree of freedom) before observation. The reason for the last assumption is discussed below. The χ-square distribution with one degree of freedom just means that the speed decrements are found by generating Gaussian random numbers, squaring, and multiplying by a scale factor. For the fall case we have assumed values of $-5\,\mathrm{km\,s^{-1}}$ for the systematic x and y components. These are just approxi-
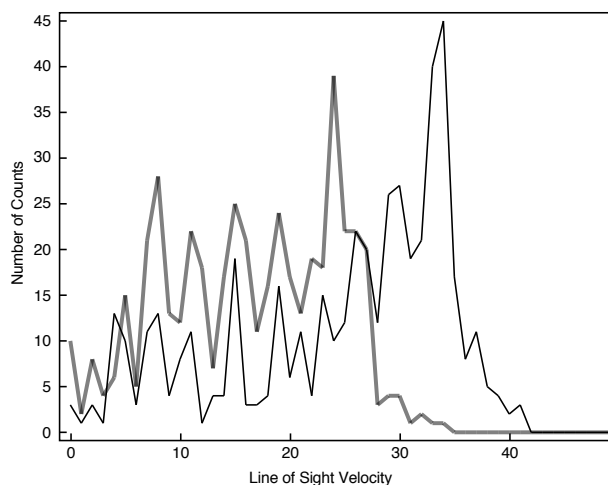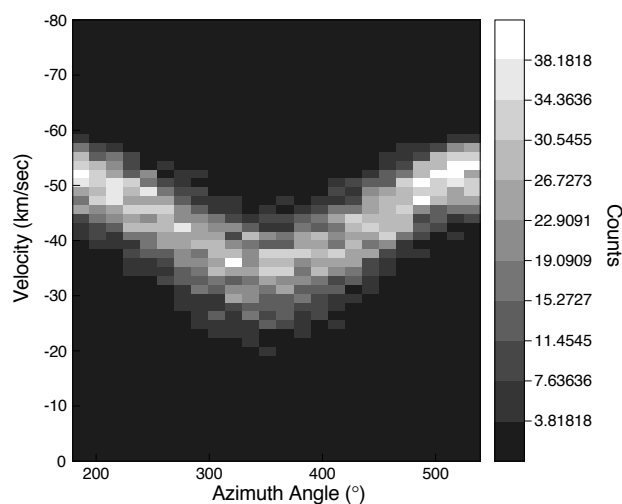

Fig. 9. A primitive model of the results shown in Fig. 7.

mate values; however, neither could be zero for the model to work. They imply that the center of the distribution is 5° east and north of the apex. We have also assumed $8\,\mathrm{km\,s^{-1}}$ for the sigmas of the Gaussian distributions, giving roughly 8° of dispersion in the direction perpendicular to the apex. We have low sensitivity at dawn in the x direction, and so that value could vary a lot. It is the y value that determines how flat the distribution is in the south, and so it matters. Finally we have assumed that the scale factor in the speed decrement is $5\,\mathrm{km\,s^{-1}}$.

As we shall see below, and as Janches et al. (2003a) has shown, there is a separate distribution of apparently slow particles, and we are not attempting to model this, or the medium speeds.
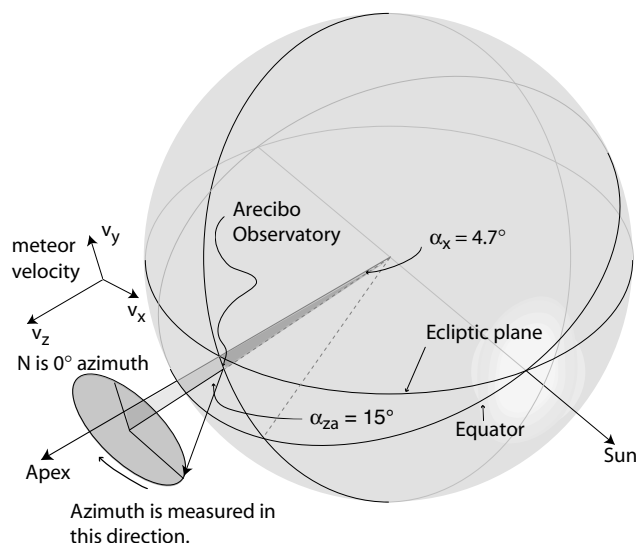
Fig. 10. Observations at the autumn Equinox.

Fig. 11. The velocities of all meteoroids on 24 September 2003 from 03:00 to 07:00 AST.

Figure 9 shows the model; although it is not perfect it does a pretty good job of reproducing the measurements near the sinusoid. It is interesting to compare this model with the one required for the fall results.

4 Fall Observations

The autumn equinox provides an opportunity to verify some of the tentative conclusions made in the last section. Figure 10 shows the relationship between the radar pointing and the apex. Note that the radar zenith points nearly along the apex at dawn, and so the azimuth track holds nearly a constant 15° angle with respect to the apex. This means that the higher frequency temporal variations seen at dawn should be very small, while structure should still be seen away from dawn, if there is alignment with the apex.

Figure 11 shows the velocity data for 24 September 2003 in the same format as Fig. 5 did for the March data. The ripples at dawn are indeed missing, and structure is visible before dawn. It has the expected low frequency component, and the paired features seen in Fig. 2 are also visible, marked by vertical arrows. Of course this apex-aligned structure in the velocity lies between north and east, and so the spacing in the close features is wider than shown in Fig. 2 for the east-west structure. (One can think of sliding the beads down the lines until the right angle is reached.)

Figure 12 shows the distribution of the velocities with azimuth angle from four days of fall equinox data (23–26 September 2003), about 8 000 total events, or roughly 4 000 meteors. (The average number of radar pulses seeing a single meteor is two.) It is equivalent to Fig. 7 for the spring; it resembles that figure in that the velocities are concentrated near $-60 \, \mathrm{km \, s^{-1}}$, but the systematic variation with azimuth
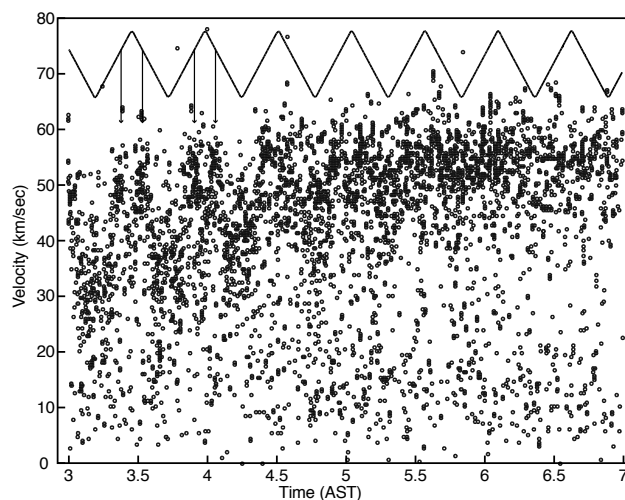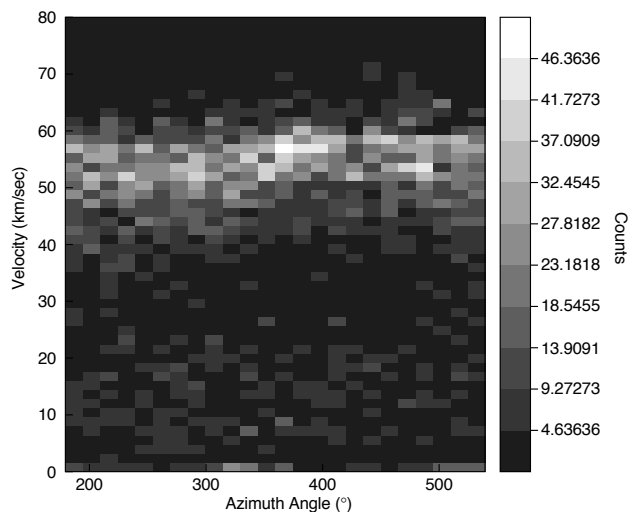
is small in this case as expected. We have removed some interference from the data from 23 September 2003 only.

Figure 13 shows the same data as Fig. 12 summed over azimuth angle. This distribution is essentially the same as Fig. 4 of Janches et al. (2003a) for the dawn time period looking south with the Gregorian feed. The radar pointing direction associated with the data of that figure is as close as possible to the pointing direction of the fall data described here. Thus the two data sets are consistent. However, it should be noted that we have not verified that all the the events are meteors, and so the the counts at the highest speeds (above the peak) might be false. Janches et al. (2003a) does not show such meteors.
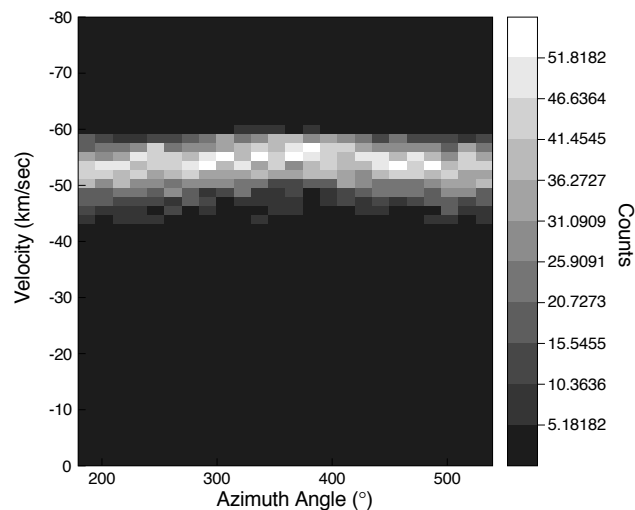
Figure 14 shows a model of the fall observations. The parameters are not identical to the spring model; the average x and y component have been set to zero. These observations are very sensitive to an average y component; the value used for the spring observations is many times too large. That is, these velocities come from right from the apex at least with respect to the y direction. The dispersions in all directions have changed from the spring model.
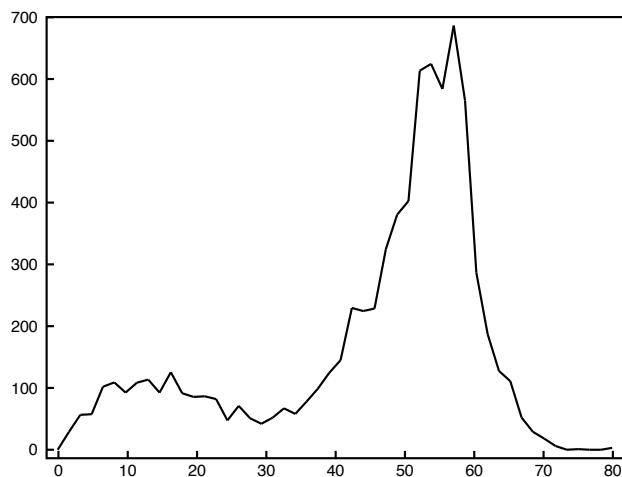
5 Disussion and Conclusions

We believe that the data and model of the two previous sections are a strong corroboration of the results of Chau and Woodman (2004), which first described the apex alignment. Some discussion is necessary, however. First, there is the matter of the slightly different directions in the spring and fall. It is not a contradiction that the directions measured are in the two seasons differ by a small amount. In the fall, the radar is located nearly in the ecliptic plane, while in the spring, it is located well above it. This is a large enough

Fig. 12. The distribution of the velocities with azimuth angle from four days of fall equinox data (23–26 September 2003).

Fig. 14. A primitive model of the results shown in Fig. 12.

Fig. 13. The distribution of the velocities summed over azimuth angle from four days of fall equinox data (23–26 September 2003).

several $km\,s^{-1}$ before observation. During the radar-visible phase of the entry of a particle, it slows by several $km\,s^{-1}$; this can be verified from this data set or others. On average, we see a particle when it is partly through its radar-visible path, because most do not come right through the center of the beam. This means that we see particles when they have slowed, and several $km\,s^{-1}$ is a reasonable number for the average lost speed. This provides the source of the downward dispersion in the magnitude of the velocity, and allows the assumption that the speeds are all very nearly the same before they enter the atmosphere.

We have explained the "down the beam" effect described in, for example, Janches et al. (2003a) and Janches et al. (2003b), as primarily a geometric effect. If one observes at dawn, and the meteors tend to come from the apex, then they will be seen to come "down the beam". If one does not know about the possibility of apex alignment and assumes that the source direction is random, then an atmospheric effect would appear to be the probable complete explanation for the alignment with the beam. Of course, we have had to assume an atmospheric effect in order to make the geometrical model work. Thus we are not saying that there are no atmospheric effects contributing to beam alignment. Indeed, all such effects will need to be included in a complete model of the process and probably will be very important.

We have made very little use of the data except in the dawn periods. Data from all seasons and all times should be used simultaneously to make a single model. This would probably involve some modern inverse technique, and it would be a lot of work. However, it would probably be the only way to include selection effects, and thus allow the possibility of examining the properties of the full population.

difference so that there could be some differences in the particle orbits that the radar sees. It is the physical position of the radar above the ecliptic that matters. We do not expect the distribution of meteors to appear any different as the pointing direction of the radar is changed with azimuth motion since the observations are only about 100 km from the surface of the earth, and so the horizontal distance from two pointing positions separated by 180° is only about 50 km.

If we make the reasonable assumption, based on the directional information measured in both the spring and the fall, that the particles are in retrograde orbits with nearly the same parameters as the orbit of the earth, then the total velocity must be $60\,km\,s^{-1}$, twice the speed of the earth in its orbit. We need to explain why we assumed an average loss of

Edited by: J. Plane

References

Chau, J. L. and Woodman, R. F.: Observations of meteor-head echoes using the Jicamarca VHF radar in interferometer mode, Atmos. Chem. Phys., 4, 511–521, 2004.

Janches, D., Nolan, M. C., Meisel, D. D., Mathews, J. D., Zhou, Q. H., and Moser, D. E.: On the geocentric micrometer velocity distribution, J. Geophys. Res., 108, 1222–1235, 2003.

Janches, D., Nolan, M. C., and Sulzer, M. P.: Radiant measurement accuracy of micrometers detected by the Arecibo 430 MHz dual-beam radar, Atmos. Chem. Phys., 4, 621–626, 2004.

Sulzer, M. P.: A radar technique for high range resolution incoherent scatter autocorrelation function measurements utilizing the full average power of klystsron radars, Radio Science, 21, 1033–1040, 1986.